MICROSCALE METROLOGY USING STANDING WAVE PROBES

Marcin B. Bauza, Shane C. Woody, Stuart T. Smith, Richard M Seugling, Ian Darnell, Jeffery N Florando

August 6, 2008

Disclaimer

MICROSCALE METROLOGY USING STANDING WAVE PROBES

Marcin B. Bauza[1], Shane C. Woody[1], Stuart T. Smith[2], Richard M. Seugling[3]
Ian M. Darnell[3] and Jeffery N. Florando[3]
[1] InsituTec Inc.
Charlotte, NC, USA
[2] UNC Charlotte
Charlotte, NC, USA
[3] Lawrence Livermore National Laboratory
Livermore, CA, USA

INTRODUCTION

Miniaturization has been one of the driving forces in the development of new technologies leading to new products in a variety of industries. As a result, the integration of components over several orders of magnitude on the length scale poses enormous challenges for quality assurance and control [1][2]. Therefore, new solutions are necessary to meet the growing need for more challenging metrology tasks and metrology requirements in nano- and micro-technology. However, with miniaturization, new challenges arise such as the increased influence of adhesion, electrostatic, Van der Waals and meniscus forces that affect the measurement process [3]-[5]. Technical solutions to overcome these micro- and nano-metrology challenges will include the need for traceability, new calibration procedures and calibration artifacts [1][6]. Over the past decade many new metrology tools have been proposed [7][8], however; for contact-based measurements, adhesion between the measurement probe and the specimen still proves to be one of the more difficult challenges to overcome [6]. To address this issue, a new class of tactile sensing probe referred to as standing wave sensor has been developed and was previously presented [9]. Previous work introduced the principle of operation of the standing wave senor. This work presents new measurements showing applications of the standing wave probe as the sensing element in a microscale high aspect ratio profiling system.

EXPERIMENTAL APPARATUS

The instrument used during the experiments presented in this work comprises an engineered gauge head that is rigidly attached to a Moore 1.5 machine frame as shown in Figure 1. The gauge head is composed of a precision spindle and scanning head which are used to position the microscale standing wave probes. The measured components are positioned with an Aerotech™ FiberMax 5 axis positioning platform. A simplified block diagram is provided below to show the reader the instrument with its multi-axis functionality, Figure 2. The *X, Y* and *Z axes* are located on the Moore 1.5 and subsequently used only for coarse alignment. Once the fiber probe and workpiece are positioned within the correct working volume of the FiberMax, the stages on the Moore 1.5 are locked and are not used during the measurement process.
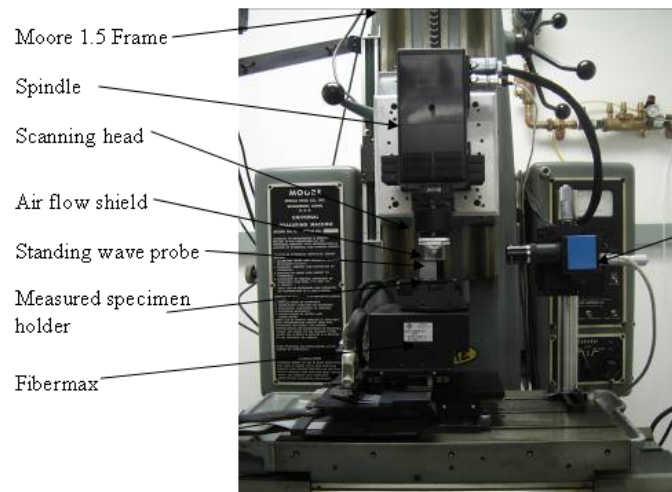

FIGURE 1. Test bed used during experiments.

There are two modes of operation reported for this work. In the first the InsituTec gauge head (configured with the spindle, sub-nanometer servoing head, and fiber probe) is used to perform roundness and cylindricity measurements. For cylindricity measurement, the FiberMax's Z-axis is used to increment the fiber probe along the axis of the hole to perform roundness traces at specified depths. This methodology for roundness scanning has previously been reported for macroscale force probes [10].

The second measurement mode addresses surface profiling for geometries that are conical, concave, and convex as well as flat surfaces. During these measurements, the precision spindle is rotated to align the standing wave probe's sensitive axis normal to the workpiece surface. Both the spindle position and the servoing head are then held at a constant position and not used during the scanning sequence. Instead, the microscale probe is only used in conjunction with the FiberMax alignment stages. During scanning, the X axis is translated while the Y-axis is used to control a constant applied force (estimated at 50 µN) between the probe tip and workpiece surface. This method results in a 2D surface plot and may be extended to 3D plots by employing the Z-axis.
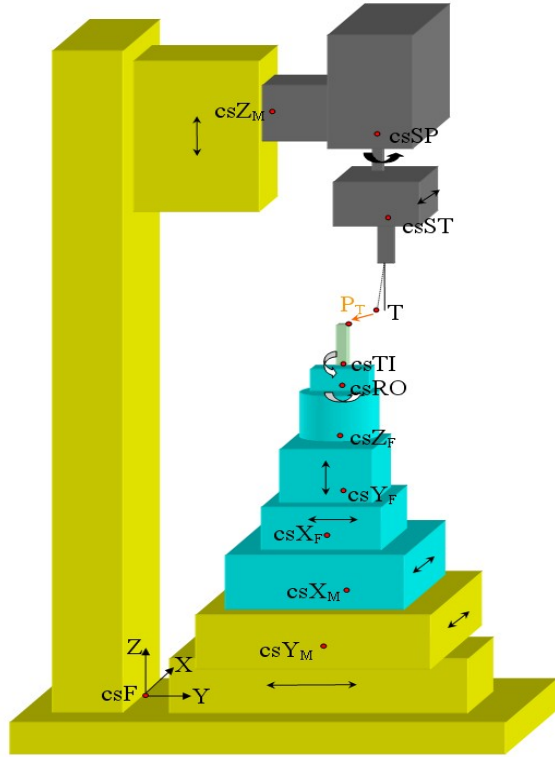

FIGURE 2. Block diagram representation of test bed used during experiments

SYSTEM ERROR MOTION ANALYSIS
To achieve better insight regarding the performance (accuracy and repeatability) of the measuring instrument, a detailed error budget has been derived. Estimates of the magnitude of the error sources are determined using the type A and B methodologies [11], vendor specifications, experimental data, and user experience. All error sources for the test-bed were assumed to be worst case and uncorrelated. In practice the combined error sources will be lower than reported. For example, the 5 axis motion control system supplied by Aerotech generates nanometer level jitter for each axis. This is due to instability in the closed loop control system. The error value given in the error budget assumes each axis oscillates at the maximum specified value at any instant in time. Most likely, all motion components produce a random oscillation which would imply a smaller error source overall. A block diagram of the system is provided in Figure 2 showing the standing wave sensor, scanning head, precision spindle, and Moore machine column and base. To calculate possible errors authors transferred the probe tip (T) from coordinate system csST into the part coordinate system csP using 11 Homogeneous Transform Matrices (HTM). The equation is shown below with values for vector P_T derived for roundness measurements shown in Table 1.

$$\overrightarrow{P_T} = H_P H_{TI} H_{RO} H_{ZF} H_{YF} H_{XF} H_{XM} H_{YM} H_F H_{ZM} H_{SP} \overrightarrow{T_{ST}}$$

TABLE 1. Tabulated error for final vector P_T based upon the system's control instability (table assumes temperature is held constant) and error motions of the axis during roundness scan.

P_{Tx}	P_{Ty}	P_{Tz}
89 nm	107 nm	3 nm

EXPERIMENTAL MEASUREMENTS
Over the past two years various artifacts have been measured including specimens made of glass, steel, aluminum, gold, and silicon. A few examples of these measurements are discussed in the following sections. Additionally, only the raw data is presented to demonstrate the fiber's capability for microscale feature measurements. Further analysis of the data referred to the measured surfaces and shapes is beyond the scope of this paper.

Fuel Injector spray hole
Fuel injectors spray holes represent one of the most challenging features in microscale metrology. Typically, the hole size ranges from 100 to 300 µm in diameter and up to few millimeters in depth. A diesel injector spray hole approximately 180 µm in diameter was selected for this study. Due to positioning limitations, the injector was fixtured to align the spray hole collinear with the fiber probe. A vertical camera with a high magnification is mounted to the gauge head housing, oriented parallel with the

spindle's rotary axis, and offset a known distance from the center axis. During the measurement, the spray hole is located using the camera then the injector is moved by the offset value to the measurement position, Figure 3. The probe is positioning into the hole, locked
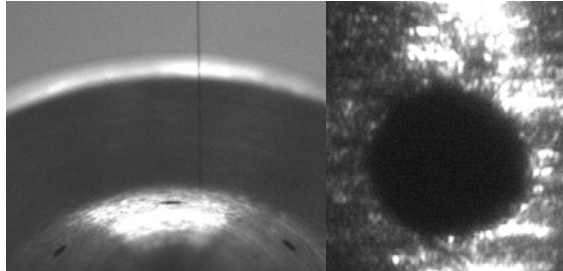

FIGURE 3. Image of a fuel injector with standing wave probe located adjacent to the hole (left), and view of the hole entrance (right).

at a constant applied force (along the hole's side wall) using the nanometer servo stage and the spindle is rotated. As the spindle is rotated, the servo stage's position is measured relative to a fixed frame on the end of the spindle, Figure 4. Each circular trace contains 1000 equispaced data points. The 3D plot is obtained by positioning the FiberMax's Z-axis to specified
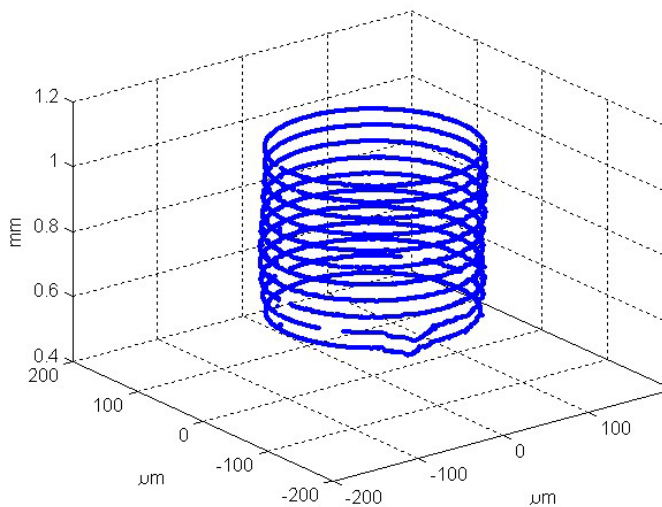

FIGURE 4. 3D representation of the fuel injector spray hole. Notice the cavity present at lower two traces, the depth of the cavity is approximately 30 μm.

depths and again measuring a circular trace. In this manner, traces equispaced by 50 μm along the depth of the hole are presented below. The data is shown in an unfiltered format with some a cavitation feature indicated in the lower portion of the hole.

Fiber optic glass ferule

Dielectric materials (i.e. glasses certain ceramics) presents another challenge due to high electrostatic forces generated on the workpiece surface. A glass ferule with a 128 μm thru diameter is manufactured with a larger tapered conical hole on the end. The alignment procedure was similar to that of the fuel injector nozzle. The glass ferule's hole was scanned twice at different sections. The first scan
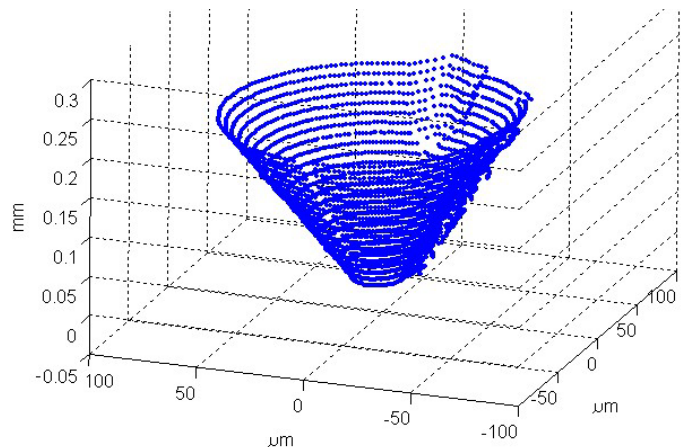

FIGURE 5. 3D representation of a conical tapered entrance to the thru hole of glass ferule. Notice the chipped surface on the back side which is approximately 20 μm deep.

represents the conically shaped entrance to the thru hole, Figure 5, and the second scan was performed deeper in the thru hole region, Figure 6. Each trace was constructed from 1000 data points and depth measurements were repeated in 10 μm increments using the FiberMax Z-axis. Imperfections of the measured surface can be seen clearly as well as the out of round shape of the ferule hole.
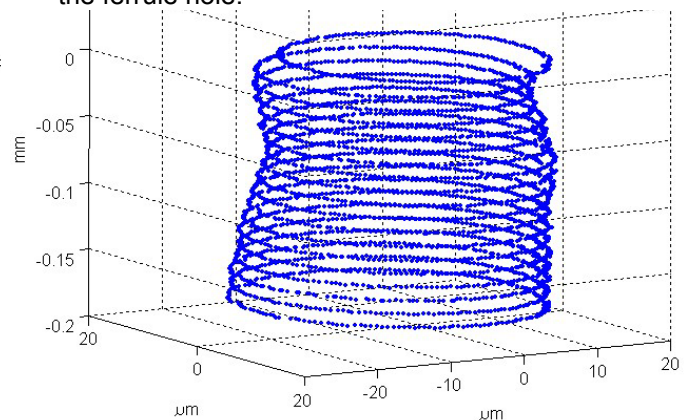

FIGURE 6. 3D representation of the 128 μm glass ferule where zero in Z corresponds to 100 μm depth.

Concave hemispherical polished surfaces

Highly polished, curved surfaces have proven to be difficult to measure using optical metrology tools. While specific methods for comparing shapes are available, these are limited to simple geometries and often require manufacture of expensive reference artifacts. More versatile optical instruments are limited by surface reflectance, materials and surface slopes. Also surface profilers and conventional CMM`s are limited due to high contact forces which can lead to scratching and surface damage. On the other hand, standing wave probes introduce low contact forces estimated to be less than 50 µN therefore significantly reducing the risk of scratching. As a case study, a highly polished steel block with conical surface and a hemispherical concave shape was measured. The dimensions of the hemispherical geometry are approximately 15 mm in diameter and 5 mm deep. The part was fixtured at 45° relative to the top of the 5 axis stage (FiberMax). Using the second mode described earlier, the part was scanned multiple times while changing the vertical height of the Z-axis, Figure 7. The data was extracted from the measurement process for each of the 10 traces.

The profile is constructed from points which are spaced 2.5 µm apart over 25 mm, and the Z-axis is stepped in by 25 µm. Due to bandwidth limitations of the Y-axis stage which is used to servo control the constant force signal it was not possible to measure surface finish. However, in principle, if a high speed gauge head similar to the one used in previous examples was used then, within the filtering limitations imposed by the fiber tip geometry, surface finish data could be obtained in addition to the surface profile.
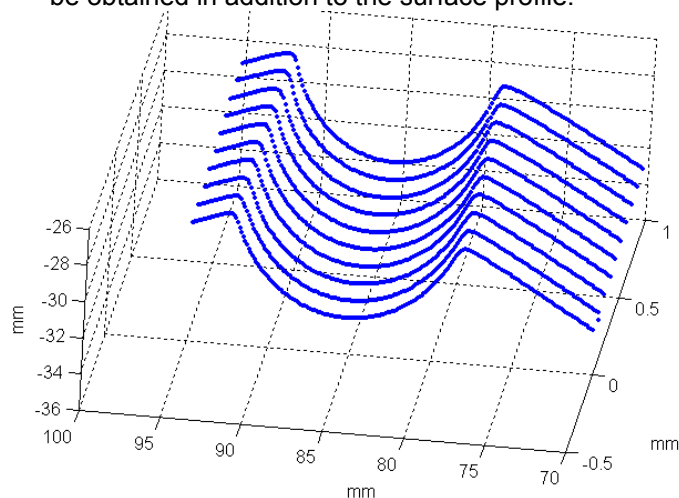

FIGURE 7. 3D representation of part of concave surface with mirror-like surface finish.

REFERENCES

[1] Hansen H.N., Carneiro K., Haitjema H., De Chiffre L., "Dimensional Micro and Nano Metrology" CIRP Annals, 55-2, 721-743 (2006)

[2] Lonardy P.M., Lucca D.A., De Chiffre L., "Emerging Trends in Surface Metrology" CIRP Annals, 51-2, 701-723 (2002)

[3] Yang, F., "Adhesive contact of axisymmetric suspended miniature structure," Sensors and Actuators A104, 44-52 (2003).

[4] Adamson, A.W. and Gast, A.P., "Physical Chemistry of Surfaces, 6th Ed.", Wiley-Interscience, (1997).

[5] Israelachvili, J.N., "Intermolecular and Surface Forces, 2nd Ed." Aca-demic Press, (1992).

[6] Marinello F., Savio E., Carmignato S., De Chiffre L., "Calibration artefact for the microscale with high aspect ratio: The fiber gauge" CIRP Annals – Manuf. Tech. 57, 497–500 (2008)

[7] Danzebrink H.-U., Koenders L., Wilkening G., Yacoot A., Kunzmann H., "Advances in Scanning Force Microscopy for Dimensional Metrology" CIRP Annals 55-2, 841–878 (2006)

[8] Weckenmann A., Peggs G., Hoffmann J., "Probing systems for dimensional micro- and nano-metrology" Meas. Sci. Technol. 17, 504–509, (2006)

[9] Bauza, M.B., Hocken, R.J., Smith, S.T., Woody, S.C., "Development of a virtual probe tip with an application to high aspect ratio microscale features," Rev. Sci. Instrum. 76, 095112 (2005)

[10] Bauza, M.B., Woody, S.C., Smith, S.T., Hocken, R.J., "Development of a Rapid Profilometer with an Application to Roundness Gauging." Precision Engineering. 30 Issue 4; 406-413, (2006)

[11] Taylor B. N., Kuyatt C. E., "Guidelines for Evaluating and Expressing the Uncertainty of NIST Measurement Results." NIST Technical Note 1297, (1994)